

Magnetic behaviour of iron–platinum alloys

P. VLAIC, E. BURZO^{a*}

University Medicine and Pharmacy “Iuliu Hatieganu”, Phys. and Biophysics Department Cluj–Napoca , Romania

^aFaculty of Physics, Babes-Bolyai University RO-400084 Cluj-Napoca, Romania

Band structure calculations were performed on disordered $\text{Fe}_x\text{Pt}_{100-x}$ alloys as well as on FePt and Fe_3Pt ordered phases. The equilibrium values of the lattice parameters, magnetic moments, Curie temperatures, pressure effects, as well as spontaneous volume magnetostrictions were obtained and compared with experimental data. It was shown that the computed values as well as the experimental data can be described starting from Néel–Slater curve. The spin glass behaviour observed in fcc $\text{Fe}_x\text{Pt}_{1-x}$ alloys, when decreasing lattice parameters, simulating the pressure effect, is also discussed.

(Received March 25, 2010; accepted May 26, 2010)

Keywords: Fe–Pt alloys, Magnetic properties, Spontaneous magnetostriction

1. Introduction

The Fe–Pt alloys system has a complex phase diagram [1,2]–Fig.1. There are three ordered phases: $L1_2$ –type for Fe_3Pt and FePt_3 and $L1_0$ type for FePt compounds. The $\text{Fe}_x\text{Pt}_{100-x}$ alloys, around the equiatomic composition ($35 \leq x \leq 55$), exhibit a typical disorder–order process, by decreasing temperature. The disordered face–centered cubic A1–type structure, having low magnetic anisotropy, orders to $L1_0$ type superstructure. In the $L1_0$ phase, the cubic symmetry is broken, due to the stacking of alternate planes of the Fe and Pt atoms, along [001] direction. The crystal structure is tetragonal having $P4/mmm$ space group. The presence of $L1_2$ phases, having $Pm\bar{3}m$ space group, can be evidenced, at room temperature, in the composition ranges $15 \leq x \leq 40$ and $68 \leq x \leq 82$. A martensitic transformation has been evidenced for composition, $x > 85$. Solid solutions of A1–type (fcc), having space group $Fm\bar{3}m$ were shown at room temperature for $x < 15$ at % and at high temperatures in all the range of compositions.

The magnetic properties of Fe–Pt alloys are closely related to chemical ordering and stoichiometry. In the composition range around FePt_3 ($15 \leq x \leq 35$), in the disordered high temperature phase, the Fe and Pt atoms occupy lattice sites randomly and a ferromagnetic type ordering has been shown. As the chemical ordering of the $L1_2$ phase progresses, the magnetic state changes from ferromagnetic to antiferromagnetic [3], a mixture of antiferromagnetic orderings [4] or a non–colinear spin structure [5,6].

The compositions close to equiatomic FePt ($44 \leq x \leq 65$) are of interest for nanoscale magnetic applications [7]. In the ordered phase, the Fe and Pt atoms form layers occupying alternating (001) planes of the original fcc lattice. The [001] direction acts as both the tetragonal symmetry

axis (*c*–axis) and easy axis of magnetization. The ordering is accompanied by a contraction along the *c*–axis, changing the *c/a* ratios from one, value characteristic for cubic symmetry. The real crystals commonly show chemical disorder with substitutions of Fe(Pt) atoms into Pt(Fe) sublattices, without changing the stoichiometry. The lattice parameters of $L1_0$ phase, in the composition range $44 \leq x \leq 65$, were studied [8]. By addition of Pt at the equiatomic composition, the *a* parameters show little change while the *c* parameters tend to be larger. The extra Pt must substantially sit on the $L1_0$ Fe sublattice which effectively will make the structure more like as a cubic phase (FePt_3), with the atomic positions in the vicinity of the defect, similar to the $L1_0$ structure. In the iron rich region ($x > 50$ at %), there is a small change in the *c*–parameter while the *a* parameter diminishes. The Fe_3Pt is cubic, having lattice parameter $a \cong 3.75 \text{ \AA}$, close to that of *c*–axis for the $L1_0$ phase (3.71 \AA). The *c/a* ratios increase from $c/a=0.966$ at FePt composition, to 0.979 ($x=65$) and 0.982 ($x=45$).

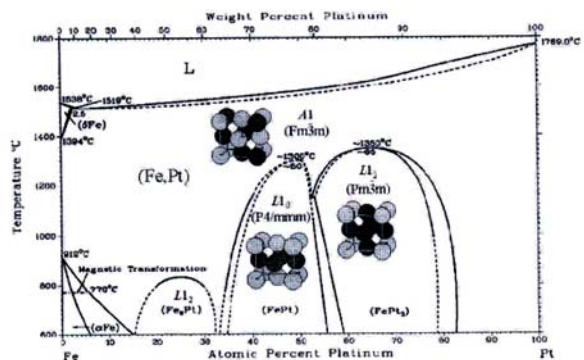


Fig.1 Phase diagram of Fe–Pt system. The crystal structures of the phases, in the different composition ranges and temperatures, are shown [1,2].

The first–principles electronic–structure calculations in FePt having tetragonal phase (L_{10}), revealed a competition between ferromagnetic and antiferromagnetic ordering of the alternating Fe planes, with energy differences less than room–temperature thermal energy [9]. The FM state is stabilized relative to AFM state, as L_{10} tetragonal distortion decreases or chemical (antisite) disorder increases in Pt planes.

The Invar effect, characterized by the absence of thermal expansion, can be seen in $\text{Fe}_x\text{Pt}_{100-x}$ alloys with 67–75 at % Fe. This effect has been shown both in chemically ordered and disordered alloys. The Invar behaviour of disordered and ordered Fe–Pt alloys were studied starting from their electronic structure [10–16]. Various methods were used to analyse this matter. More recent studies treated the paramagnetic state by using the disordered local moment (DLM) approach [11]. The calculated values were shown to describe rather well the experimental evidence [17,18].

The effect of pressure on the magnetic properties of the Fe–Pt Invar alloys were studied [19–21]. This matter has been also theoretically analysed [22]. It was shown that as lattice constants are diminished, simulating the pressure effect, the effective magnetic interactions change from ferromagnetic to antiferromagnetic in Invar region of Pt–Fe solid solutions. Thus, a spin glass phase can be shown under high pressure, at a volume slightly higher than the critical volume where the alloy becomes “nonmagnetic”.

In the present report, the physical properties of $\text{Fe}_x\text{Pt}_{100-x}$ alloys are discussed. The magnetic properties of the fcc $\text{Fe}_x\text{Pt}_{100-x}$ disordered alloys, as will be shown, can be well described in a model involving the exchange interactions dependent on the distances between iron atoms. As the lattice parameters decrease, reflecting the pressure effects, a transition to a spin glass and/or to an antiferromagnetic state is suggested. The model can explain also the magnetic behaviour of Fe–Pt ordered compounds.

2. Computational method

The ground state electronic structure, total energies, densities of states (DOS) and magnetic properties of α – and γ – $\text{Fe}_x\text{Pt}_{100-x}$ disordered alloys as well as of Fe_3Pt and FePt ordered compounds have been studied by means of spin–polarized and scalar relativistic tight–binding linear muffin–tin orbital method (TB–LMTO) within atomic sphere approximation (ASA) [23], together with the coherent potential approximation (CPA) [24]. The local spin density approximation (LSDA) was used for the exchange correlation potential of the electron gas, assuming Vosko–Wilk–Nussair parameterization [25]. The initial electronic configurations were taken as $\text{core}+3d^64s^2$ for Fe and $\text{core}+5d^{10}$ for Pt. The structures of α – and γ –phases

were assumed to be bcc (A2) and fcc (A1), respectively. The Wigner–Seitz radii of Fe and Pt constituents have been considered to be equal for disordered compounds and different for ordered ones. A spd–basis set has been used for both atoms. All band structure calculations have been performed using a mesh of $24 \times 24 \times 24$ \mathbf{k} –points in the full Brillouin zone (BZ), resulting in 413 \mathbf{k} points in the irreducible wedge of BZ, that ensure the accuracy of the total energy, better than 10^{-2} mRy. The magnetic disorder has been analysed within DLM formalism [24], by treating the binary compounds as pseudoternary $\text{Fe}_{x-c}^{\uparrow}\text{Fe}_c^{\downarrow}\text{Pt}_{100-x}$ alloys, with (x–c) atoms having spin–up state and c atoms being in the state with spin down. The DLM configuration with $c=0$ will describe the ferromagnetic (FM) ground state, while that with $c=x/2$ has been considered as a paramagnetic (PM) state, which shows no magnetic ordering. Really, this state is antiferromagnetic, in which the antiparallel alignment of magnetic moments are compensated, miming the PM state. In the composition range $35 \leq x \leq 55$ at % Fe, a disordered fcc–type structure has been considered, in agreement with the reported lattice parameters [27] or a previous theoretical study [10].

3. Results

3.1 Lattice parameters

Total energy calculations have been performed on fcc and bcc $\text{Fe}_x\text{Pt}_{100-x}$ disordered alloys in the whole composition range, in both ferromagnetic and non–magnetic states.

The total energies, E_{tot} , of the magnetic and of the non–magnetic solid solutions, as a function of lattice constants, are given in Figs.2a–d, for $\text{Fe}_{90}\text{Pt}_{10}$, $\text{Fe}_{80}\text{Pt}_{20}$ (bcc), and $\text{Fe}_{75}\text{Pt}_{25}$, $\text{Fe}_{25}\text{Pt}_{75}$ (fcc) compositions. For fcc solid solutions, at lower values of the lattice constants, the total energies are degenerate. When increasing the lattice constants, the FM state is stabilized. For fcc studied alloys, stable solutions with magnetizations, $M=0$, at lower volumes, as well as stable solutions with finite magnetization, M , at larger volumes, are evidenced. In case of bcc solid solutions the ferromagnetic state is stable in the region $0.80 \leq a/a_e \leq 1.2$, where a_e is the equilibrium lattice constant.

The equilibrium values of the lattice parameters have been determined from a polynomial fit of the total energy values. The replacement of Fe atoms by Pt ones results in an increase of the equilibrium lattice spacing. The calculated lattice constants are somewhat different from the experimentally determined values, only in the composition range $x < 40$ as well as for $x \geq 84$ –Fig.2d. The slight differences between the two sets of data can be attributed to the scalar relativistic approximation used in the present calculations.

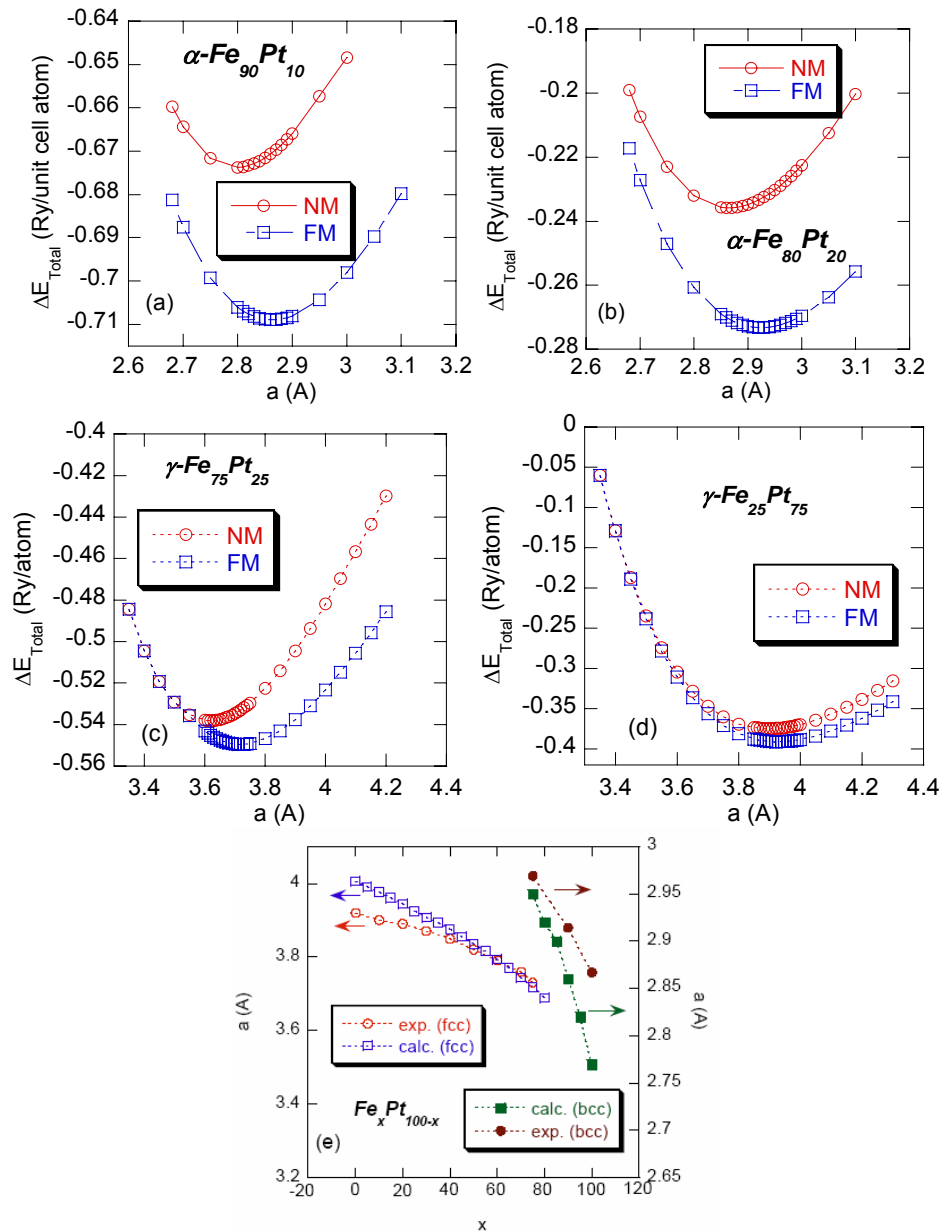


Fig.2. Total energies as function of lattice spacing for $\text{Fe}_{90}\text{Pt}_{10}$ (a), $\text{Fe}_{80}\text{Pt}_{20}$ (b) having bcc type structure and for $\text{Fe}_{75}\text{Pt}_{25}$ (c) and $\text{Fe}_{25}\text{Pt}_{75}$ (d) having fcc type structure. In (e) are shown the composition dependences of computed lattice parameters as well as experimentally determined values [27].

The matter of differences between the experimental and calculated lattice constants has been discussed [28]. Correct results, from band structure calculations, based on experimental lattice constants can be also obtained. Thus, in case of YCo_2 compound a realistic electronic structure calculation with a fully self consistent procedure has been considered in order to solve the corresponding multi-orbital Hubbard Hamiltonian. A many-body solver was used which is a modified version of the fluctuating exchange approximation which takes into account fluctuations in the particle-particle and particle-hole channel for the

multi-orbital case. Since the method involves long computation time, we used only the procedure described in section 2, for determining equilibrium lattice parameters.

3.1 Magnetic moments

The atom-resolved spin polarized density of states (DOS) for $\text{Fe}_x\text{Pt}_{100-x}$ solid solutions with $x=90,80,75$ and 25 at % are given in Fig.3. Smooth DOS are shown, due to chemical disorder that smeared the electronic states. The iron atoms exhibit a strong ferromagnetism with almost

completely filled majority spin sub-bands.

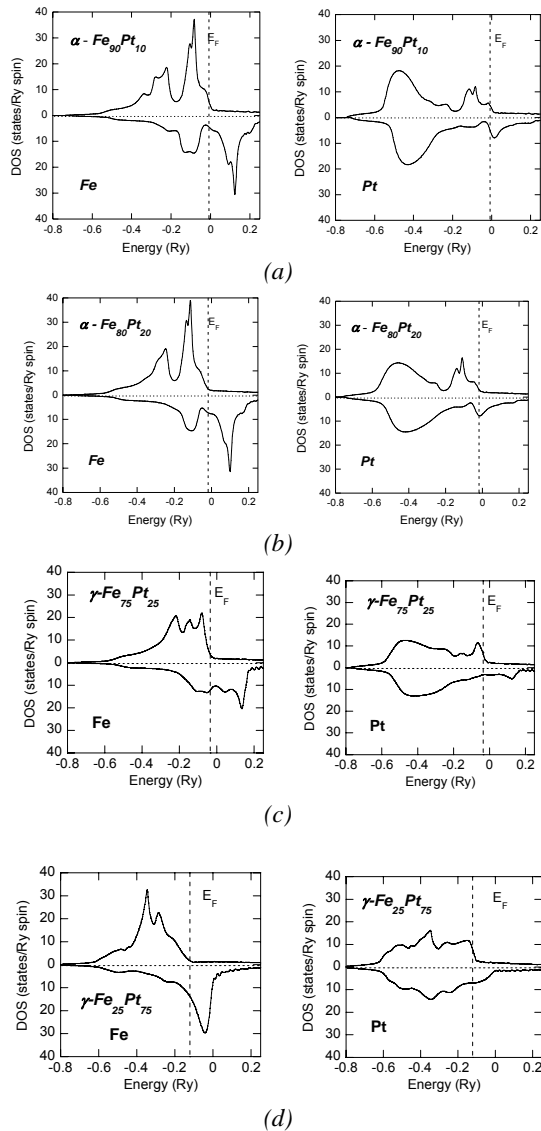


Fig.3. Atom projected DOS at Fe and Pt atoms for Fe_xPt_{100-x} having bcc (a) $x=0.90$, (b) $x=0.80$ and fcc (c) $x=0.75$, (d) $x=0.25$ type structures.

The energy states, at the Fermi level, are mostly of minority spin character. A polarization of Pt5d band, parallelly oriented to iron moment, is shown. This behaviour can be correlated with the exchange interactions of Fe3d–Pt5d type. As result of hybridization of Pt5d band with Fe3d one, the Pt5d band is split. Their splitting can be correlated with the intensity of exchange interactions, the number of Fe atoms situated in the neighbour of Pt site, respectively. This is evidenced by an increase of the a Pt magnetic moment in fcc solid solutions, particularly in the composition range $5 < x < 25$ at %, up to $0.28 \mu_B/\text{atom}$. The polarizations become nearly saturated and of $0.30 \mu_B/\text{atom}$ for higher iron content. For bcc solid solutions, the Pt5d band polarization is of $\approx 0.50 \mu_B/\text{atom}$ —Table 1.

Analysing the evolution of the minimum in the total energy curves, in case of fcc solid solutions for non-magnetic state, as function of composition—Fig.2—it can be shown that at $x_c=85$ at % Fe this is almost equal with the total energy corresponding to ferromagnetic state. This composition corresponds to non-magnetic-ferromagnetic transition. The x_c value, thus obtained, is higher than the previous reported one, namely $x_c=76$ [10]. We note that the latter value has been obtained by using the fixed spin moment method. In this method, the magnetic moment is fixed and the spin splitting is determined by self consistent calculations.

The composition dependences of the iron and platinum magnetic moments, at the equilibrium lattice constants, as well as the average magnetizations per formula unit are shown in Fig.4. In fcc type solid solutions there is an increase of iron moment per atom, as the Pt content is higher, from $2.6 \mu_B/\text{atom}$ ($x=80$) to $3.2 \mu_B/\text{atom}$ ($x=5$). Since the iron moments are nearly one order of magnitude higher than the platinum contribution to magnetization, the magnetic moment per formula unit will increase, as function of iron content. The computed moments per formula unit agree with experimental data up to $x=50$ at % Fe. Then, the calculated values are somewhat higher than the experimental values [27,29]. In bcc type solid solutions the same trend as above is observed for iron moments although these show a greater decrease. The Pt5d band polarizations are only little dependent on composition. The average magnetization has a maximum located at $x \approx 90$ at %.

Table 1. Computed magnetic moments.

Compound	Crystal structure	Lattice constants		Atom	l	m_l (μ_B)	m_{total} ($\mu_B/atom$)	M ($\mu_B/f.u.$)	
		calc.	exp.					calc.	exp.
$Fe_{90}Pt_{10}$	$Im\bar{3}m$	2.863	2.914	Fe(2a)	0	-0.003	2.492	2.292	
					1	-0.044			
					2	2.539			
				Pt(2a)	0	-0.008	0.488		
					1	-0.058			
					2	0.554			
$Fe_{80}Pt_{20}$	$Im\bar{3}m$	2.924	2.950	Fe(2a)	0	0.000	2.653	2.210	
					1	-0.038			
					2	2.691			
				Pt(2a)	0	-0.009	0.439		
					1	-0.053			
					2	0.501			
$Fe_{75}Pt_{25}$	$Fm\bar{3}m$	3.718	3.73	Fe(4a)	0	-0.008	2.606	2.025	1.81
					1	-0.044			
					2	2.658			
				Pt(4a)	0	-0.019	0.281		
					1	-0.060			
					2	0.360			
$Fe_{50}Pt_{50}$	$Fm\bar{3}m$	3.836	3.84	Fe(4a)	0	0.001	2.839	1.574	1.48
					1	-0.026			
					2	2.864			
				Pt(4a)	0	-0.014	0.308		
					1	-0.044			
					2	0.366			
$Fe_{25}Pt_{75}$	$Fm\bar{3}m$	3.925	3.88	Fe(4a)	0	0.012	3.034	1.000	0.94
					1	-0.003			
					2	3.025			
				Pt(4a)	0	-0.008	0.322		
					1	-0.025			
					2	0.355			
Fe_3Pt	$Pm\bar{3}m$	3.645	3.727	Fe(3c)	0	-0.005	2.297	7.141	6.45
					1	-0.031			
					2	2.333			
				Pt(1a)	0	-0.025	0.250		
					1	-0.086			
					2	0.361			
$FePt$	$P4/mmm$	a=3.815 c/a=0.981	a=3.861 c/a=0.981	Fe(1a/1c)	0	-0.004	2.728	6.244	5.62
					1	-0.014			
					2	2.746			
				Pt(2e)	0	-0.015	0.394		
					1	-0.065			
					2	0.474			

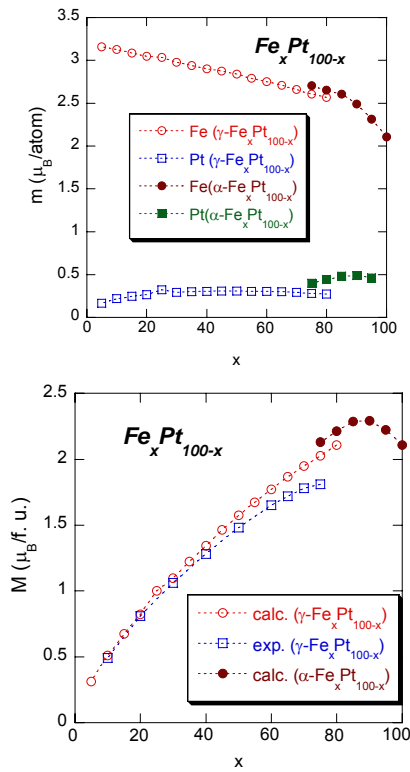


Fig.4 Composition dependences of the iron and platinum magnetic moments at the equilibrium lattice constants, as well as of the average magnetizations per formula unit. The experimentally determined values [29] of magnetization, at 4.2 K, are also given.

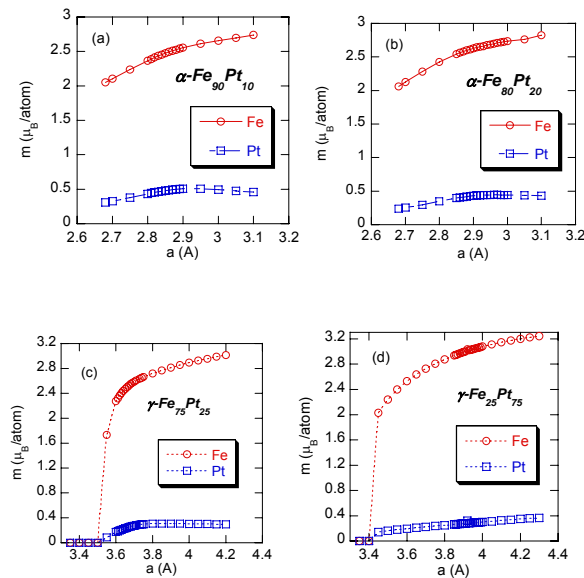


Fig.5 The dependences of iron moments and of Pt 5d band polarizations on lattice constants for bcc ($\text{Fe}_{90}\text{Pt}_{10}$ (a), $\text{Fe}_{80}\text{Pt}_{20}$ (b)) and fcc ($\text{Fe}_{75}\text{Pt}_{25}$ (c), $\text{Fe}_{25}\text{Pt}_{75}$ (d)) solid solutions.

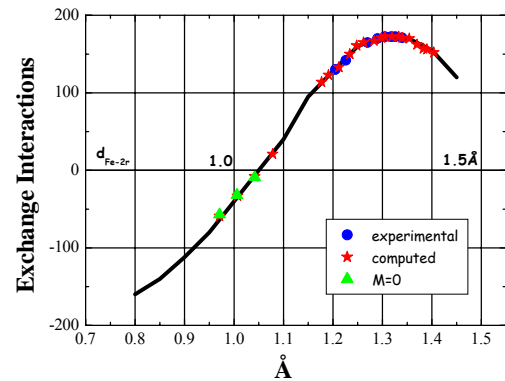


Fig. 6. The Néel–Slater curve describing the exchange interactions as function of d_{Fe} , the distances between iron atoms. The determined distances d_{Fe} in case of $\text{Fe}_x\text{Pt}_{100-x}$ alloys are also plotted.

The dependences of the iron moments and of platinum 5d band polarizations on the lattice parameters, simulating the pressure effect, in $\text{Fe}_{25}\text{Pt}_{75}$, and $\text{Fe}_{75}\text{Pt}_{25}$ fcc and $\text{Fe}_{80}\text{Pt}_{20}$, $\text{Fe}_{90}\text{Pt}_{10}$ bcc alloys, are given in Fig.5. Analysing the Fig.2, can be seen, that in fcc solid solutions at lower lattice constants, the total energies of ferromagnetic and “non-magnetic” states are degenerate and there are stable solutions for $M=0$. As a result, a “nonmagnetic” state can be stable at high pressures, for a critical value, a_c , of lattice parameter. Values $a_c=3.50 \text{ \AA}$ ($x=75$), 3.45 \AA ($x=50$) and 3.40 \AA ($x=25$) were evidenced. These correspond to reductions of lattice parameters, from equilibrium values, at 89.3 %, 90.8 % and 91.1 % for compositions $x=0.75$, 0.50 and 0.25, respectively. The above behaviour can be correlated with the distances between the iron atoms, d_{Fe} . According to Néel [30], the exchange interactions are dependent on d_{Fe} values—Fig.6. Neglecting the contributions of Pt atoms to the exchange interactions, the Fe3d-Fe3d interactions will decrease both by increasing or decreasing the distances between iron atoms from the value situated at $s=d_{\text{Fe}}-2r=1.36 \text{ \AA}$ where r is the iron radius (0.72 \AA). The exchange interactions are negative for $s < 1.05 \text{ \AA}$, leading to antiferromagnetic type ordering. The lattice parameters of $\text{Fe}_x\text{Pt}_{100-x}$ fcc alloys corresponding to “non-magnetic” state suggest that d_{Fe} values are situated slightly below, the region where the presence of negative exchange interactions is expected.

The presence of negative exchange interactions between iron atoms, when the $d_{\text{Fe}} < 2.50 \text{ \AA}$ ($s < 1.06 \text{ \AA}$), has been evidenced in rare-earth (R)–iron compounds, as R_2Fe_{17} and $\text{R}_2\text{Fe}_{14}\text{B}$ [31–34]. Thus, for very short distances between iron atoms, a helicoidal arrangement of the iron magnetic moments was shown in R_2Fe_{17} compounds with $\text{R}=\text{Lu}$, crystallizing in hexagonal $\text{P6}_3/\text{mmc}$ space group. In case of R_2Fe_{17} with $\text{R}=\text{Y}, \text{Gd}$ or of $\text{R}_2\text{Fe}_{14}\text{B}$ compounds, the latter having $\text{P4}_2/\text{mmm}$ -type structure, there are different iron sites in lattice, the distances between them covering a large range of values. The negative exchange interactions between some iron, situated in sites located at $d_{\text{Fe}} < 2.50 \text{ \AA}$,

are not satisfied since the positive ones, with atoms located at larger distances, are more intense. Consequently, a large magnetic energy is stored. The competition between elastic and magnetic energies leads to anomalies in thermal dilatation as Invar effect and a decrease of Curie temperatures [32–34].

The transition to a “non-magnetic” state takes place at smaller critical lattice parameters a_c , as the Pt content increases. This fact can be correlated with the iron content and their statistical distribution in lattice sites. In case of smaller fraction of iron atoms, these can be situated also at larger distances than expected if all iron occupy randomly lattice sites. Consequently, a higher decrease of the lattice constants is required to induce a “non-magnetic” state, as evidenced from band structure calculations.

Pressure studies were performed on some Fe–Pt Invar alloys [19–21]. In case of disordered $\text{Fe}_{70}\text{Pt}_{30}$ composition, the Curie temperature decreased with increasing pressure [19]. Also the ferromagnetism of this alloy becomes weaker and antiferromagnetic interactions become dominant. The above behaviour is the same as predicted by Néel–Slater curve. In case of bcc alloys ($x > 75$ at %), the ferromagnetic state is stable for the range of lattice constants $0.80 \leq a/a_e \leq 1.20$, where a_e is the equilibrium lattice constant. No transition to nonmagnetic state was shown.

The exchange interactions in the fcc $\text{Fe}_x\text{Pt}_{100-x}$ disordered alloys were evaluated, in the mean field approximation, from the differences between the total energy of the FM and DLM states. The maximum in the composition dependence of the exchange interactions in the present report, is located at $x \cong 60$ at % Fe – Fig.7. These follow a similar dependence as predicted by the Néel–Slater curve, although the maximum in the last case can be seen for a lattice constant $a \cong 3.90 \text{ \AA}$, that corresponds to $x \cong 55$ at % Fe.

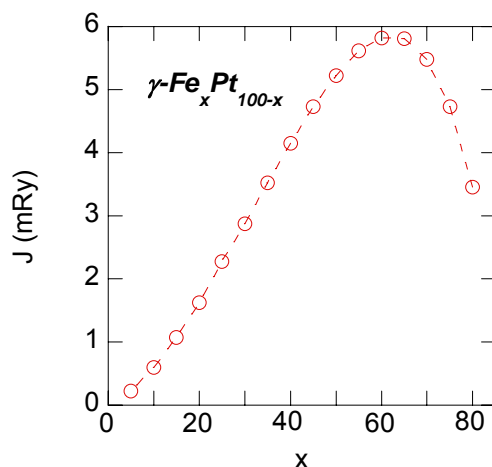


Fig. 7. The exchange coupling constants in fcc $\text{Fe}_x\text{Pt}_{100-x}$ disordered alloys.

The composition dependence of the computed Curie temperatures, T_C , for fcc solid solutions are given in Fig.8. As expected, these follow the same trend as the exchange interactions. The experimental T_C values follow similar

variation as computed ones, but the maximum is shifted to compositions having somewhat lower iron content. These are near superposed on computed values when translated by $\cong 5$ at % Fe.

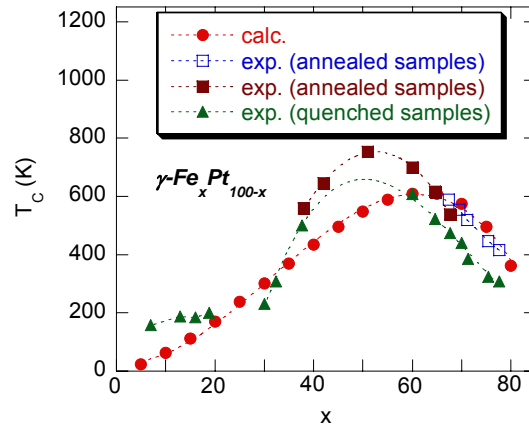


Fig.8. Composition dependence of the Curie temperatures, T_C . The experimentally determined values [29] are also given.

3.3 Spontaneous volume magnetostriction

The spontaneous volume magnetostriction, ω_s , is defined as the relative volume difference between the magnetically ordered and paramagnetic (DLM) phase. The composition dependence of the ω_s values has been analysed in Fe–Pt Invar alloys by using DLM method [10,11,16]. The spontaneous volume magnetostriction, ω_s , has been defined in terms of the ratio between the difference of the equilibrium volumes for the ferromagnetic and DLM states and the volume of FM state [11]:

$$\omega_s = \frac{V(\text{FM}) - V(\text{DLM})}{V(\text{FM})}$$

Referring to Fig.2, as already discussed, there are two minima of the total energy versus lattice parameters, corresponding to magnetic ordered and paramagnetic DLM state, respectively. The spontaneous volume magnetostriction can be shown in a magnetically ordered alloy for which the paramagnetic DLM minimum with a small lattice constant (small magnetic moment) is slightly above the magnetic solution with a larger lattice constant. When increasing temperature, the local minimum with small lattice constant can be populated by thermal fluctuations which counteracts the usual thermal expansion due to lattice vibrations [10]. Néel [30] attributed the above anomaly, to the magnetic energy variation as function of the volume, the distances between atoms, respectively, as result of the magnetic coupling energies between the spins. Also he showed that the anomaly, ω_s , at the magnetic transition temperature, is proportional to the square of the magnetization.

The computed composition dependence of the ω_s values are shown in Fig.9. The maximum value can be evidenced for a composition $x \cong 75$ at %. The computed ω_s values, are little greater ($\cong 0.3$ %), although close to those experimentally determined [17,18], as well as on those previously theoretically computed [10,11,16]. We note that high values of the spontaneous volume magnetostriction are shown for compositions having lattice exchange constants close to the region of transition from positive to negative ones, on Néel–Slater curve.

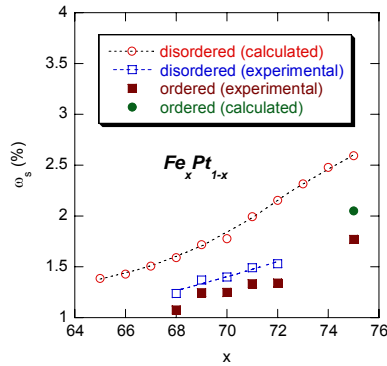


Fig. 9. Composition dependence of the spontaneous volume magnetostriction. The experimental values [29] are also given.

As previously showed [16], the maximum of ω_s corresponds to an electron concentration per atom $e/a=8.5$, so called magic electronic number—Fig.10a.

Néel [30], suggested that the ω_s values are linearly dependent on the difference between the square of the magnetic moments of magnetic and paramagnetic states. According to Khmelevskiy et al [16], this effect can be explained also in terms of the electronic band structure. The gain in the kinetic energy of the valence electrons, due to band splitting, is partially counter-balanced by an increase in the volume. Since the magnetic moments are determined by band splitting, the ω_s values will be proportional to the volume. It is thus expected that the magneto–volume coupling scales linearly with the difference between the squares of the magnetic moments. The above prediction [16,30] is fulfilled as can be seen in Fig.10b.

The crystallographic and magnetic properties of Fe_3Pt and FePt ordered compounds were also analysed. The total energy, as function of lattice parameters for Fe_3Pt and of volume variation for FePt , respectively are given in Fig.11. In Fig.12 the computed magnetic moments of Fe and Pt atoms are plotted as function of lattice parameters. In case of Fe_3Pt , a transition to a non-magnetic state is shown at $a_c \cong 3.55$ Å. The corresponding distance between iron atoms is $d_{\text{Fe}}=2.51$ Å and $s=1.07$ Å, respectively. On the Néel–Slater curve, this is situated near the point where the positive exchange interactions vanish, the negative ones prevailing for slightly lower distances between iron atoms.

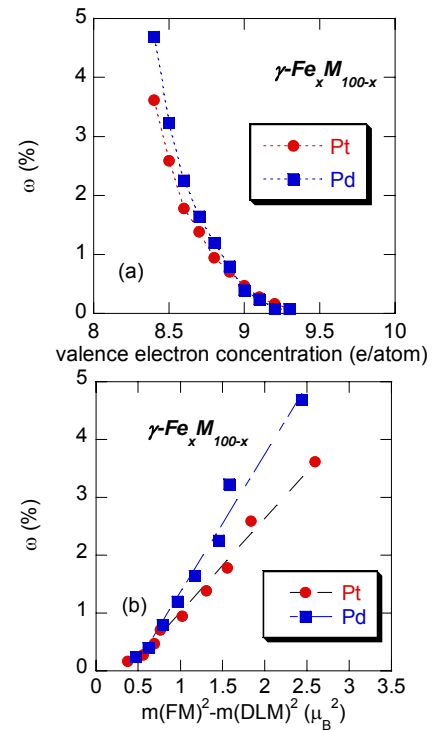


Fig.10. The ω_s values for $\text{Fe}_x\text{M}_{100-x}$ with $M=\text{Pt}$ and Pd as function of electron concentration (a) and of the difference between the square of the magnetic moments (b).

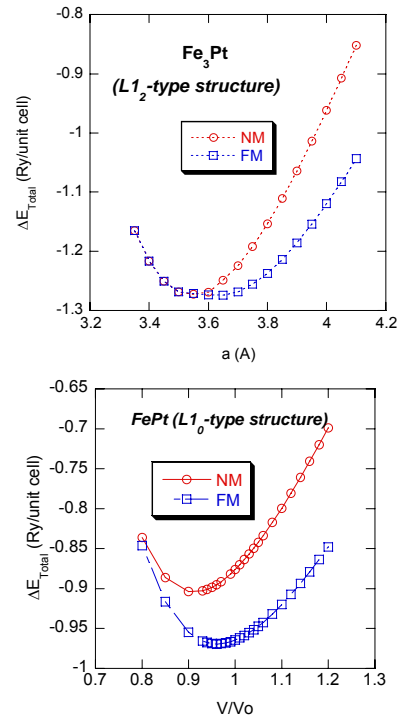


Fig.11 Total energy for FM and NM states as function of lattice parameters (Fe_3Pt) and volumes (FePt).

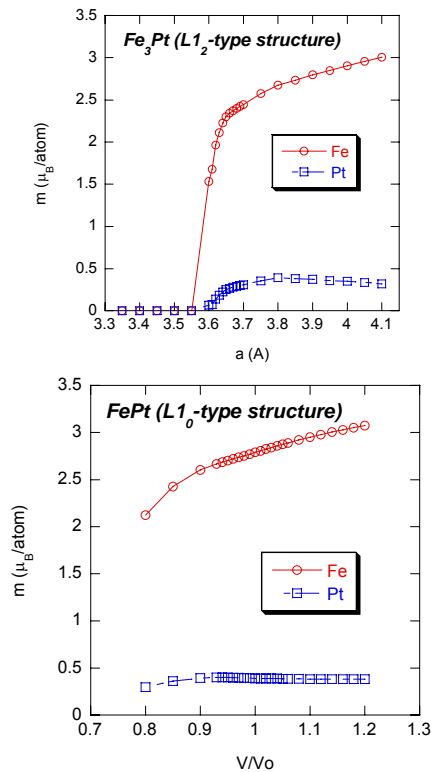


Fig.12. The computed magnetic moments on Fe and Pt atoms as a function of lattice parameters for Fe_3Pt and of volumes for $FePt$.

The pressure effect has been studied in case of ordered $Fe_{72.8}Pt_{27.2}$ alloy [21]. A new high-pressure magnetic phase appeared, at 3.5 GPa, in the low temperature range. This phase has been shown to be more ferromagnetic rather than antiferromagnetic or spin glass. No indication of crystal structure or lattice parameters has been given. Consequently, we speculate that in the above ordered alloy, there is a distortion of crystal structure as effect of pressure and as a result the distances between iron atoms are probably distributed in a range of values. These are expected to correspond to atoms located at both $s < 1.06$ Å and > 1.06 Å, respectively. There is a possibility that negative exchange interactions involving Fe atoms situated at $d_{Fe} < 2.50$ Å ($s < 1.06$ Å) to be relatively small as compared to positive ones, and consequently a ferromagnetic type behaviour, as observed for example in $Y_2Fe_{14}B$ -based compounds, can be shown [33]. A considerable magnetic energy is stored, having as effect a diminution of Curie temperature.

The $FePt$ compound shows a tetragonal structure, where two types of iron atoms are present. The Fe(1a) site has, in the first coordination shell, 4Fe(1c) atoms situated at 2.73 Å and in the second one 2Fe(1a) at 3.788 Å and 4Fe(1a) at 3.861 Å. The variation of the Fe magnetic moment, simulating the pressure, as showed in Fig.12, evidence no transition to a non magnetic state for $V/V_0 \geq 0.8$.

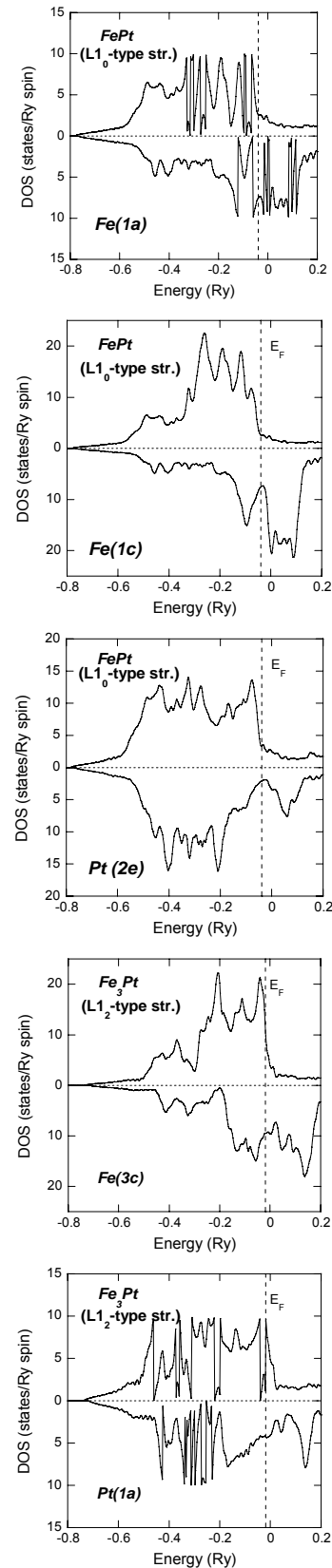


Fig. 13. Density of states for $FePt$ (a,c) and Fe_3Pt (d,e), at equilibrium lattice constants.

Since we have two types of iron sites, situated at different distances, the exchange interactions are more complex than in cubic structure. By reducing volume, as effect of pressure, the Fe(1a)–Fe(1c) exchange interactions can be negative. The exchange interactions between Fe(1a) atoms must remain positive, since these atoms are situated at 1.4 times longer distances than between Fe(1a)–Fe(1c) ones. Since of the greater number of iron atoms, of Fe(1a) type involved in positive exchange interactions, the possible negative ones are not satisfied and consequently this system remains ferromagnetic. Similar behaviour was shown in R_2Fe_{17} ($R=Y, Gd$) compounds [33,34].

The atom resolved spin polarized density of states (DOS), determined at equilibrium lattice constants for Fe_3Pt and $FePt$, are given in Fig.13. The majority spin sub-bands are almost filled, the states at the Fermi level having mainly spin minority character. The Fe3d magnetic moment is higher in $FePt$ compound than in Fe_3Pt one. Due to Fe3d–Pt5d exchange interactions, the Pt5d band is split. The Pt5d band polarizations are parallelly oriented to iron moment and higher in $FePt$ compound as compared to Fe_3Pt one. This can be connected with higher iron magnetic moments of atoms involved in the exchange interactions with Pt5d ones as evidenced in $FePt$ compound. The magnetic moments per formula unit agree rather well with experimental data as showed in Table 1.

The computed spontaneous magnetostriction is of 2.06 %, close to the value obtained experimentally in Fe_3Pt ordered alloy (1.77 %).

4. Conclusions

The total energy calculations on Fe_xPt_{100-x} disordered alloys were analyzed for ferromagnetic, non-magnetic and paramagnetic DLM states. A transition from ferromagnetic to a non-magnetic state has been shown for fcc type structures at $x_c=85$. The iron magnetic moments decrease when the Pt content diminishes. A Pt5d band polarization is induced by Fe3d–Pt5d bands hybridization. The Curie temperatures of fcc solid solutions were computed. These follow a similar composition dependence as experimental values, but their maximum is shifted by ≈ 5 at % Fe in the iron rich region.

The magnetic properties have been analysed as function of lattice parameters, simulating the effect of pressure. At high pressures, involving a decrease of lattice parameters, to $a/a_c \approx 0.9$, a spin glass type behaviour is suggested in fcc type alloys, as experimentally evidenced. No evidence of magnetic–non magnetic transition was shown in bcc Fe_xPt_{100-x} alloys for $a/a_c \geq 0.9$. The effect of competition between negative and positive exchange interactions, determined by the presence of both short (<2.50 Å) and larger (>2.50 Å) distances between iron atoms, on the magnetic properties is discussed. The spontaneous volume magnetostrictions, ω_s , were evidenced for fcc disordered alloys having $65 \leq x \leq 75$ at % Fe. The ω_s values scale linearly as function of differences between the squares of magnetic moments of ferromagnetic and paramagnetic states. The above behaviour can be

correlated also with the electron concentration and lattice parameters. In this composition region the distances between iron atoms, determined from lattice constants, are only somewhat higher than the value $d_{Fe} \approx 2.50$ Å, characteristic for the possible presence of negative exchange interactions. In case of Fe_3Pt compound a value ω_s was evidenced, close to that experimentally determined in ordered phase.

Acknowledgements

Realized also in the grant 71-060 with the Acronim APLIMAG.

References

- [1] T. B. Massalski, Binary Alloys Phase Diagram, ASM International, Materials Park, OH, USA, 1992
- [2] O. Gutfleisch, J. Lyubina, K. H. Müller, L. Schultz, *Adv. Mat. Eng.* **7**, 208 (2005)
- [3] G. E. Bacon, J. Crangle, *Proc. Roy. Soc. London A* **272**, 387 (1963)
- [4] N. Tobita, N. Nakajima, N. Ishimatsu, H. Maruyama, K. Shimada, H. Namatame, M. Taniguchi, *J. Phys. Soc. Jpn.* **79**, 024703 (2010)
- [5] Y. Tsunoda, R. Abe, *Phys. Rev.* **B55**, 11507 (1997)
- [6] Y. Tsunoda, D. Tsuchia, Y. Higashiyama, *J. Phys. Soc. Jpn.* **72**, 713 (2003)
- [7] S. Sun, C.B. Murray, D. Weller, L. Folks, A. Moser, *Science* **287**, 1989 (2000)
- [8] T. J. Klemmer, N. Shukla, C. Liu, X. W. Wu, E. B. Svedberg, O. Mryasov, R. W. Chantrell, D. Weller, M. Tanase, D. E. Laughlin, *Appl. Phys. Lett.* **81**, 2220 (2002)
- [9] G. Brown, B. Kraczek, A. Janotti, T. C. Schulthess, G. M. Stocks, D. D. Johnson, *Phys. Rev.* **B68**, 052405 (2003).
- [10] R. Hayn and V. Drchal, *Phys. Rev.* **58**, 4341 (1998)
- [11] B. Khmelevskiy, A. V. Ruban, Y. Kakehashi, P. Mohn, B. Johansson, *Phys. Rev.* **B72**, 064510 (2005)
- [12] Zs. Major, S. B. Dugdale, T. Jarlborg, E. Bruno, B. Ginatempo, J. B. Staunton, J. Poulter, *J. Phys.: Condens. Matter.* **15**, 3619 (2003)
- [13] M. Uhl, L. M. Soudratskii and J. Kübler, *Phys. Rev.* **B50**, 291 (1994)
- [14] M. Podgorny, *Phys. Rev.* **B46**, 6293 (1992)
- [15] V. Crisan, P. Entel, M. Ebert, H. Akai, D. D. Johnson J. B. Staunton, *Phys. Rev.* **B66**, 014416 (2002)
- [16] S. Khmelevskiy, I. Turek, P. Mohn, *Phys. Rev. Letters*, **91**, 037201 (2003)
- [17] E. F. Wassermann, *Phys. Scripta* **T25**, 209 (1989); *Ferromagnetic Materials*, Ed. K. H. J. Buschow, E. P. Wohlfarth, North Holland, **5**, 237 (1990).
- [18] M. Shiga in *Material Science and Technology*, Ed. R. W. Cahn, P. Haasen and E. J. Kramer, VCH, Verlagsgesellschaft, Weinheim, **3b**, 159 (1994).
- [19] M. Matsushita, S. Endo, K. Miura, F. Ono, *J. Magn. Magn. Mat.* **260**, 371 (2003)

- [20] M. Matsushita, S. Endo, K. Miura, F. Ono, J. Magn. Magn. Mat. **284**, 403 (2004)
- [21] M. Matsushita, S. Endo, M. Miura, F. Ono, J. Magn. Magn. Mat. **269**, 393 (2004)
- [22] S. Khmelevskiy, P. Mohn, Phys. Rev. **B68**, 214412 (2003)
- [23] O. K. Anderson and O. Jepsen, Phys. Rev. Letters **53**, 2571 (1984)
- [24] I. Turek, V. Drchal, J. Kudrnovsky, M. Sob, P. Weinberger, Electronic Structure of Disordered Alloys, Surfaces and Interfaces, Kluwer Academic, Boston, 1997
- [25] S. H. Vosko, L. Wilk, M. Nusair, Can. J. Phys. **58**, 1200 (1980)
- [26] A. J. Pindor, J. B. Staunton, G. M. Stocks, H. Winter J. Phys. F.: Metal Phys. **13**, 979 (1983)
- [27] V. L. Sedov, Antiferromagnetism of γ -Fe. The Invar Problem, Nauka, Moscow, 1987
- [28] L. Chioncel, E. Burzo, J. Optoelectron. Adv. Mater. **8**, 1105 (2006)
- [29] J. J. M. Franse, R. Gersdorf, in Landolt Börnstein Handbook, Vol. 19, Srpinger Verlag, Berlin, 1986, p.566
- [30] L. Néel, Ann. Physique **8**, 237 (1937)
- [31] D. Givord, R. Lemaire, I.E.E.E Trans. Magn. **10**, 109 (1974)
- [32] E. Burzo, Reports Progr. Phys. **61**, 1099 (1998); E. Burzo, W. Kappel, M. Codescu, E. Helerea, J. Optoelectron. Adv. Mater. **11**, 229 (2009)
- [33] E. Burzo, L. Stanciu, W. E. Wallace, J. Less Common Met. **111**, 83 (1985); A. T. Pedziwiatr, W. E. Wallace, E. Burzo, V. Pop, Solid State Commun. **61**, 61 (1987); E. Burzo, V. Pop, N. Plugaru, L. Stanciu, W. E. Wallace, Solid State Commun. **58**, 803 (1986)
- [34] M. Valeanu, N. Plugaru and E. Burzo, Solid State Commun. **89**, 519 (1994).

*Corresponding author: burzo@phys.ubbcluj.ro